

# Carbon-13 NMR Investigation of Spin-Lattice Relaxation Mechanism of Poly(4-methyl-1-pentene)

SUN MA,\* M.-C. CHEN, and S.-P. WANG

Institute of Chemistry, National Cheng Kung University, Tainan, Taiwan 701, Republic of China

## SYNOPSIS

Carbon-13 spin-lattice relaxation rates ( $1/T_1$ ) and nuclear Overhauser enhancement (NOE) measurements were performed on poly(4-methyl-1-pentene) above the glass transition temperature in order to explain the segmental motion of the molecule by means of high-resolution nuclear magnetic resonance spectroscopy. Experiments were carried out for poly(4-methyl-1-pentene) with low, medium, and high molecular weights. The similarity of the  $T_1$  values showed that for polymers with a degree of polymerization (DP) > 100 the relaxation behavior of the carbon atoms no longer depends on molecular weight. The temperature effects were studied at 358, 363, 373, 383, 393, and 403 K, both on 25.18 and 100.61 MHz magnetic fields. Finally, several mathematical  $T_1$  models were applied to study the change of  $T_1$  encountered by the individual carbon atoms. The results reveal that the more factors being considered in the calculation the more consistent will be the results obtained with the  $T_1$  model. A comparison showed that parameters used in the DLM  $T_1$  model gives the best fit. © 1994 John Wiley & Sons, Inc.

## INTRODUCTION

The study of dynamic properties of macromolecules by means of  $^{13}\text{C}$ -nuclear magnetic resonance (NMR) spectroscopy has become one of the most promising methods in recent years.<sup>1-15</sup> A number of studies focused on the measurement of spin-lattice relaxation times and the nuclear Overhauser enhancement for polymers in solution in order to calculate the correlation time  $\tau_c$  for the segmental motions of the bulky side chain of the molecule.

In this project, we intended to study poly(4-methyl-1-pentene) by means of high-resolution NMR techniques. Poly(4-methyl-1-pentene) is a well-known material for an oxygen-enriched membrane; the permeability of oxygen of this polymer is considered higher than that of other materials. The bulky side-chain rotation could have increased the free volume of the polymer, and, therefore, increased the permeability. Since the segmental motion along the chain determines the molecular transport

through the membrane, the relaxation time constant  $T_1$  of the carbon atoms can provide a direct insight into the membrane permeability in these systems. Therefore, it is interesting to carry out a thorough relaxation study for the carbon atoms in order to investigate the local side-chain motion of poly(4-methyl-1-pentene). However, this research is confined to the study of the polymer dissolved in a deuterated solvent at temperatures higher than 358 K; it is impossible to reflect the molecular motion in the solid state.

The present work was performed above the glass transition temperature,  $T_g$ , of the polymer. Below the  $T_g$ , the polymer exists in the solid state and the bonding chains are hindered for fast motions; as a result, the dipolar coupling interaction between carbon and hydrogen atoms and the contribution from the chemical-shift anisotropy cannot be averaged out effectively. Consequently, the NMR signals obtained are significantly broadened.<sup>16-18</sup>

For polymers above the  $T_g$ , the motions are so fast that the dipolar coupling interaction and the chemical-shift anisotropic effects are averaged out to a large extent; therefore, well-resolved signals can be obtained.<sup>19,20</sup>

\* To whom correspondence should be addressed.

In the present work, the  $^{13}\text{C}$ -NMR spectrum of poly(4-methyl-1-pentene) was measured and the chemical shifts assigned. Spin-lattice relaxation time constants  $T_1$  and nuclear Overhauser enhancements (NOE) were performed to interpret the segmental motions of the polymer. Experiments were carried out for low, medium, and high molecular weights for different temperatures with 400 and 100 MHz FT-NMR instruments.

Hall and Helfand,<sup>21</sup> Viovy et al.,<sup>22</sup> Jones and Stockmayer,<sup>23</sup> and Skolnick and Yaris<sup>24</sup> proposed in their works mathematical models describing the segmental motions of the side chains of the polymer. They tried to find a set of parameters that are consistent with the experimental results. Furthermore, they studied the temperature effects on  $T_1$  values of the nuclei and the line shape of the relevant signals. We have applied these models to our system and compared the results obtained for a thorough understanding of the segmental motion of our system.

## EXPERIMENTAL

### Material and Sample Preparation

Poly(4-methyl-1-pentene) labeled with low, medium, and high molecular weights were purchased from Aldrich Chemical Co. and used without further purification. The glass transition temperatures,  $T_g$ , were determined with a Thermal Analyst 2000, which are 12, 23, and 43°C for low, medium, and high molecular weights, respectively. All solutions were prepared in 5 mm o.d. NMR sample tubes with 0.14 g poly(4-methyl-1-pentene) in 0.79 g 1,1,1,2,2-tetrachloroethane (99.5% D, bp = 146°C, purchased from Fluka Chemical Co.); the final percentage weights are 15% for all three samples. The sample tubes were degassed by the freeze-thaw method. Since the polymer did not dissolve at room temperature, the tubes were heated in an oil bath (110°C) for 1 week; after cooling down, a condensed homogeneous gel can be obtained, which was degassed three times by freeze-thaw and sealed for measurement.

### NMR Measurements

$^{13}\text{C}$ -NMR measurements were done at two frequencies, namely, 25.18 MHz (by a BRUKER WP-100 NMR spectrometer) and 100.61 MHz (by a BRUKER AMX-400 NMR spectrometer). Experiments were performed at 358, 363, 373, 383, 393, and 403 K using the inversion-recovery method for the spin-

lattice relaxation time constants of the carbon atoms. Every experiment was repeated twice. The standard deviations of the  $T_1$  values for all temperatures are less than 5% except for 358 K. Broadband decoupling and inverse-gated decoupling methods were also carried out for the evaluation of the NOE enhancements, and the temperature calibration was made for a 80% glycol solution.

## RESULTS AND DISCUSSION

The carbon-13 spectrum is shown in Figure 1. The assignment of the chemical shifts is quite straightforward and can be found in the literature. Since it is not of interest in this study, we only presented the results.

When analyzing the spin-lattice relaxation rate, we have to consider all possible relaxation mechanisms: The overall relaxation rate is the sum of six types of the relaxation mechanisms, namely, the dipole-dipole relaxation,  $R_{1DD}$ ; the chemical-shift anisotropic relaxation,  $R_{1CSA}$ ; the spin rotation relaxation,  $R_{1SR}$ ; the quadrupolar relaxation,  $R_{1Q}$ ; the paramagnetic relaxation,  $R_{1P}$ ; and the scalar coupling relaxation,  $R_{1SC}$ .

In our experiment, quadrupole nuclei and paramagnetic substances are not present; therefore,  $R_{1Q}$  and  $R_{1P}$  can be neglected. Moreover, the contribution of  $R_{1SC}$  is also negligibly small due to the difference of Larmor frequencies between carbon and hydrogen nuclei. In our system, the overall relaxation rate can be given by

$$R_1 = R_{1DD} + R_{1CSA} + R_{1SR} \quad (1)$$

The  $^{13}\text{C}$ — $^1\text{H}$  dipolar relaxation rate,  $R_{1DD}$ , is inversely proportional to the  $r^6$ , and  $r$  is the interdistance between carbon and hydrogen atoms. From the nuclear Overhauser effect, it is known that

$$R_{1DD} = \frac{\eta_{\text{obs}}}{\eta_{\text{max}}} R_1 \quad (2)$$

which can be expressed in terms of relaxation times:

$$T_{1DD} = \frac{\eta_{\text{max}}}{\eta_{\text{obs}}} T_1 \quad (3)$$

$\eta_{\text{obs}}$  is the experimental value for NOE. If the relaxation is completely contributed by the  $^{13}\text{C}$ — $^1\text{H}$  dipolar interaction,  $\eta_{\text{max}} = 1.989$ .

Table I represents the  $T_1$  values for 25.18 and 100.61 MHz. Table II lists the corresponding NOEs.

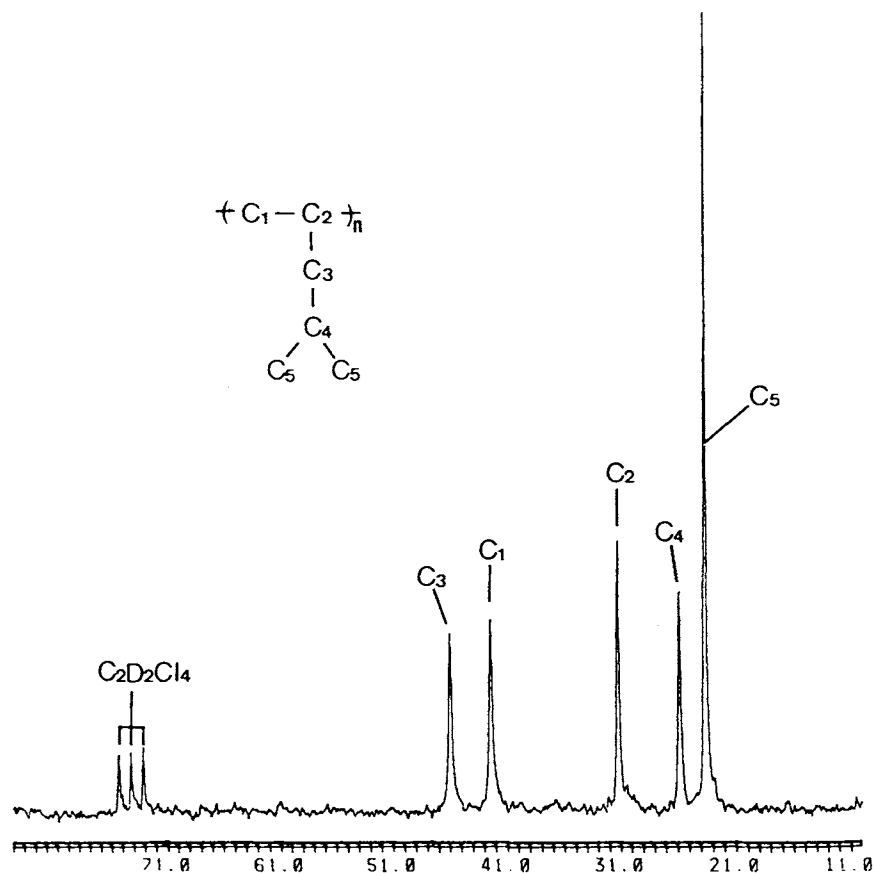


Figure 1 The carbon-13 spectrum of poly(4-methyl-1-pentene).

From these data, the <sup>13</sup>C — <sup>1</sup>H dipolar relaxation time constants,  $T_{1DD}$ , for all five carbon atoms at the measured temperatures can be obtained.

The contribution of chemical-shift anisotropy,  $R_{1CSA}$ , can be expressed as

$$R_{1CSA} = \frac{1}{T_{1CSA}} = \frac{2}{15} \gamma^2 H_0^2 (\delta_{\parallel} - \delta_{\perp})^2 \tau_c \quad (4)$$

where  $\delta_{\parallel}$  and  $\delta_{\perp}$  are the shielding tensors parallel and perpendicular to the molecular symmetry axis.

As can be seen,  $R_{1CSA}$  increases quadratically with the strength of the magnetic field. Where the spin rotation  $R_{1SR}$  is independent of the field strength,

$$R_{1SR} = \frac{1}{T_{1SR}} = \left( \frac{2\pi IKT}{h^2} \right) C^2 \tau_{SR} \quad (5)$$

From eq. (1), the sum of  $R_{1CSA}$  and  $R_{1SR}$  can be calculated quite straightforwardly. Since our experiments were performed on both 400 and 100 MHz NMR instruments, and the 400 MHz field strength

is 3.99563 times stronger than the 100 MHz, therefore,

$$R_{1CSA} (100.61 \text{ MHz}) = 15.965 R_{1CSA} (25.18 \text{ MHz}) \quad (6)$$

However, the spin rotation relaxation rates remain constant at different magnetic fields if the temperature is kept constant. Therefore, combining the results yields the following equation:

$$\begin{aligned} & (R_{1CSA} (100.61 \text{ MHz}) + R_{1SR} (100.61 \text{ MHz})) \\ & - (R_{1CSA} (25.18 \text{ MHz}) + R_{1SR} (25.18 \text{ MHz})) \\ & = 14.965 R_{1CSA} (25.18 \text{ MHz}) \quad (7) \end{aligned}$$

$R_{1CSA} (25.18 \text{ MHz})$  and  $R_{1CSA} (100.61 \text{ MHz})$  can be easily evaluated with eqs. (6) and (7). Since spin-rotation is independent of the magnetic field, therefore,  $T_{1SR}$  can be obtained quite straightforwardly. The results of  $T_{1DD}$ ,  $T_{1CSA}$ , and  $T_{1SR}$  of the polymer

**Table I** The Spin-lattice Relaxation Time Constants  $T_1$  for All Carbon Atoms of Poly-(4-methyl-1-pentene)

Frequency MHz	MW	C	358 K	363 K	373 K	383 K	393 K	403 K
25.18	L	C1	65.3	74.6	89.8	104.3	132.3	139.0
		C2	110.1	126.7	157.2	182.7	219.1	234.0
		C3	81.1	86.2	101.8	113.9	143.3	153.8
		C4	184.5	196.0	234.7	260.0	326.6	352.2
		C5	590.1	740.4	824.0	968.4	1238.1	1330.1
		C2/C1	1.69	1.70	1.75	1.75	1.67	1.68
		C4/C3	2.27	2.27	2.30	2.28	2.28	2.29
25.18	M	C1	63.1	72.1	90.9	106.2	119.8	141.6
		C2	109.3	124.7	152.5	179.7	196.2	233.4
		C3	76.2	80.9	104.4	126.5	138.5	153.8
		C4	176.8	188.6	236.3	297.2	318.6	349.5
		C5	592.6	737.2	895.2	1067.8	1274.9	1303.7
		C2/C1	1.73	1.73	1.68	1.69	1.64	1.65
		C4/C3	2.32	2.33	2.26	2.35	2.30	2.27
25.18	H	C1	64.9	72.1	85.1	101.4	114.9	125.0
		C2	113.5	124.8	143.0	165.0	190.0	210.0
		C3	79.4	86.1	99.2	107.5	124.0	129.4
		C4	182.6	199.5	226.4	245.2	281.5	295.0
		C5	605.0	698.2	800.2	934.2	1062.3	1154.5
		C2/C1	1.75	1.73	1.68	1.63	1.65	1.68
		C4/C3	2.30	2.32	2.28	2.28	2.27	2.28
100.61	L	C1	153.2	173.0	197.4	208.5	231.9	255.0
		C2	275.5	302.5	335.0	355.3	401.8	440.5
		C3	207.2	221.1	253.6	262.5	304.3	332.2
		C4	504.4	538.8	607.8	648.8	734.1	756.6
		C5	1083.5	1167.8	1426.8	1518.3	1852.0	2021.5
		C2/C1	1.80	1.75	1.70	1.70	1.73	1.73
		C4/C3	2.43	2.44	2.39	2.47	2.41	2.28
100.61	M	C1	171.9	179.7	191.7	210.0	223.9	248.2
		C2	292.2	312.8	350.4	366.2	390.0	418.5
		C3	204.1	224.0	248.2	275.1	290.8	318.4
		C4	529.4	564.5	601.1	645.1	693.1	746.3
		C5	1134.0	1241.5	1387.8	1597.8	1769.8	1986.0
		C2/C1	1.70	1.74	1.83	1.74	1.74	1.69
		C4/C3	2.59	2.52	2.42	2.34	2.38	2.34
100.61	H	C1	164.2	177.2	191.3	212.1	237.5	257.5
		C2	286.4	300.1	323.6	362.2	402.8	433.3
		C3	204.9	221.6	238.6	269.5	302.6	325.5
		C4	495.8	521.4	601.3	638.2	697.9	748.8
		C5	1085.0	1182.5	1353.0	1559.0	1787.0	1973.5
		C2/C1	1.74	1.69	1.69	1.71	1.70	1.68
		C4/C3	2.42	2.35	2.52	2.37	2.31	2.30

L, M, and H represent polymers with low, medium, or high molecular weight measured in ms.

with medium-sized molecular weight for all the measured temperatures are presented in Table III.

From the experiments performed at 25.18 MHz, the relative contributions of  $R_{1DD}$ ,  $R_{1CSA}$ , and  $R_{1SR}$  to the total spin-lattice relaxation are given in Table

IV. It is obvious that the principal relaxation mechanism undergone by our system is the  $^{13}\text{C}-^1\text{H}$  dipolar relaxation rate;  $R_{1DD}$  is more than 93%. The percentage for  $R_{1SR}$  is less than 1%. This result shows that for carbon atoms of poly(4-methyl-1-

**Table II** The NOE for All Carbon Atoms of Poly-(4-methyl-1-pentene)

Frequency MHz	MW	C	358 K	363 K	373 K	383 K	393 K	403 K
25.18	L	C1	1.880	1.887	1.886	1.901	1.920	1.931
		C2	1.879	1.890	1.899	1.912	1.931	1.942
		C3	1.853	1.863	1.870	1.887	1.903	1.927
		C4	1.863	1.871	1.873	1.886	1.896	1.898
		C5	1.956	1.956	1.958	1.961	1.958	1.964
25.18	M	C1	1.883	1.889	1.891	1.913	1.935	1.931
		C2	1.881	1.893	1.897	1.923	1.938	1.940
		C3	1.851	1.867	1.867	1.876	1.901	1.927
		C4	1.867	1.870	1.875	1.871	1.881	1.903
		C5	1.950	1.953	1.957	1.957	1.960	1.965
25.18	H	C1	1.883	1.891	1.890	1.908	1.928	1.937
		C2	1.873	1.880	1.901	1.923	1.937	1.948
		C3	1.846	1.865	1.877	1.876	1.915	1.936
		C4	1.860	1.867	1.879	1.891	1.885	1.897
		C5	1.950	1.951	1.951	1.957	1.961	1.963
100.61	L	C1	1.152	1.124	1.154	1.232	1.340	1.390
		C2	1.022	1.100	1.218	1.284	1.408	1.506
		C3	0.988	1.020	1.066	1.202	1.246	1.292
		C4	0.992	1.002	0.972	1.036	1.138	1.174
		C5	1.544	1.588	1.606	1.620	1.616	1.648
100.61	M	C1	1.038	1.060	1.166	1.270	1.348	1.398
		C2	1.078	1.097	1.148	1.294	1.434	1.494
		C3	0.961	1.010	1.062	1.154	1.236	1.316
		C4	1.010	0.974	1.008	1.030	1.068	1.148
		C5	1.504	1.535	1.608	1.598	1.635	1.668
100.61	H	C1	1.100	1.102	1.145	1.208	1.289	1.380
		C2	1.036	1.117	1.165	1.278	1.397	1.496
		C3	0.939	0.983	1.078	1.113	1.228	1.312
		C4	1.016	1.038	0.991	1.056	1.085	1.118
		C5	1.534	1.550	1.589	1.607	1.627	1.646

pentene) at low magnetic fields (25.18 MHz) the spin-lattice relaxation mechanism is due mainly to the dipole-dipole interaction between carbon and hydrogen nuclei.

For experiments performed at 100.61 MHz, the contribution of the dipole-dipole relaxation is still the dominant mechanism used.  $R_{1DD}$  is between 48 and 84%. But the percentage of the relaxation rate from the chemical-shift anisotropy has increased to 15–37%.

### Molecular Weight

It can be shown<sup>25,26</sup> that in the case of polymer in solution the spin-lattice relaxation times,  $T_1$ , are independent of molecular weight if the degree of polymerization (DP) is higher than 100. In our experiments, although three polymer samples have dif-

ferent molecular weights, DP values are larger than 100. Therefore, the  $T_1$  values depend only on the segmental motion of the polymer. Similar  $T_1$  results were obtained for low, medium, and high molecular weights regardless of the fields and temperature used (Table I).

### Magnetic Field Strength

For  $\omega\tau_C > 1$  and for the same  $\tau_C$ ,  $T_{1DD}$  increases with the Larmor frequency of the measured nuclei if temperature is kept constant. Helfand<sup>27</sup> derived the following equation for the polymer chain:

$$\tau_c \approx \eta C \exp(E^*/RT) \quad (8)$$

where  $\eta$  is the viscosity, and  $C$ , the molecular constant.  $E^*$  is the activation energy of motion. It is

**Table III** The  $T_{1DD}$ ,  $T_{1CSA}$ , and  $T_{1SR}$  for All Carbon Atoms of Poly(4-methyl-1-pentene) of Medium Molecular Weight

Frequency MHz	Type	C	358 K	363 K	373 K	383 K	393 K	403 K
25.18	$T_{1DD}$	C1	66.7	75.9	95.6	110.4	123.1	145.9
		C2	115.6	131.0	159.9	185.9	201.4	239.3
		C3	81.9	86.2	111.3	134.1	144.9	158.7
		C4	188.4	200.6	250.7	315.9	336.9	365.3
		C5	604.5	750.8	909.8	1084.7	1293.8	1319.6
100.61	$T_{1DD}$	C1	329.4	337.2	326.9	328.9	330.3	353.1
		C2	539.1	567.2	607.1	562.8	541.0	557.1
		C3	422.5	441.1	464.7	474.1	468.0	481.2
		C4	1042.5	1152.7	1186.2	1246.1	1290.9	1293.0
		C5	1499.7	1608.7	1716.6	1988.9	2153.2	2368.2
25.18	$T_{1CSA}$	C1	7.73	7.87	9.27	10.99	12.34	15.10
		C2	13.97	14.30	16.56	19.44	25.59	30.59
		C3	9.22	10.40	11.62	13.87	15.23	17.40
		C4	25.67	25.50	25.91	27.27	30.07	33.79
		C5	82.25	93.94	124.65	142.35	167.86	207.85
100.61	$T_{1CSA}$	C1	0.48	0.49	0.58	0.69	0.77	0.95
		C2	0.87	0.90	1.04	1.22	1.60	1.92
		C3	0.58	0.65	0.73	0.87	0.95	1.09
		C4	1.61	1.60	1.62	1.71	1.88	2.12
		C5	5.15	5.88	7.81	8.92	10.51	13.02
100.61 25.18	$T_{1SR}$	C1	1.40	1.75	2.30	3.72	6.87	7.16
		C2	2.35	3.15	4.12	7.51	10.92	13.73
		C3	1.25	1.51	1.99	2.66	3.94	6.89
		C4	3.25	3.60	4.89	6.14	7.29	10.62
		C5	47.77	71.92	100.53	131.75	181.73	224.78

Units:  $T_{1DD}$  in ms;  $T_{1CSA}$  and  $T_{1SR}$  in s.

evident that, if the concentration, solvent, and temperature are kept constant,  $\tau_C$  will not be affected by the magnitude of the field strength.  $T_{1DD}$  increases with the strength of the external magnetic field for  $\omega\tau_C \geq 1$ .  $T_{1CSA}$ , on the contrary, is inversely proportional to the square of the field strength. Finally,  $T_{1SR}$  is independent of the magnetic field.

### Temperature Effect

As can be seen from Table III, the  $T_{1DD}$  values increase with temperature. If the temperature is raised, the rapid molecular tumbling places them in the extreme narrowing condition, where  $\tau_C$  is small and  $T_{1DD}$  is inversely proportional to the correlation time,  $\tau_C$ .

According to eq. (4),  $T_{1CSA}$  is inversely proportional to  $(\delta_{\parallel} - \delta_{\perp})^2 \cdot \tau_C$ . As temperature increases, the molecular motions become faster and the shielding tensors  $\delta_{\parallel}$  and  $\delta_{\perp}$  can be partially averaged

out and the term  $(\delta_{\parallel} - \delta_{\perp})^2$  is small. Therefore, it is evident that at higher temperatures  $T_1$  values increase. The experimental results are shown Table III.

Since the  $T_{1SR}$  value is independent of the magnetic field strength, the  $T_{1SR}$  obtained with 25.18 and 100.61 MHz are equal for constant temperature. For temperatures above the vaporization point,  $T_{1SR}$  is inversely proportional to  $T$ ,  $C^2 \tau_{SR}$ , where  $C$  is the average spin-rotation tensor.<sup>28,29</sup> However, as can be seen from Table III, the  $T_{1SR}$  increases with temperature. This can be explained by that all the temperatures used in this work are still below the vaporization point, where  $\tau_{SR}$  decreases with temperature.

In this work, tetrachloroethane was used as the reference, with the central signal set at  $\delta$  74.36 ppm. Table V lists the chemical shift of carbon atoms for all the measured temperatures. In our experiment, the electron shielding tensor is the only factor that

**Table IV** The Percentage of  $R_{1DD}$ ,  $R_{1CSA}$ , and  $R_{1SR}$  in All Carbon Atoms of Poly(4-methyl-1-pentene) of Medium Molecular Weight

		358 K	363 K	373 K	383 K	393 K	403 K
<u>25.18 MHz</u>							
C1	$R_{1DD}$	94.67	94.98	95.07	96.18	97.29	97.08
	$R_{1CSA}$	0.82	0.92	0.98	0.97	0.97	0.94
	$R_{1SR}$	4.51	4.12	3.95	2.85	1.74	1.98
C2	$R_{1DD}$	94.57	95.17	95.38	96.69	97.43	97.54
	$R_{1CSA}$	0.78	0.87	0.92	0.92	0.77	0.76
	$R_{1SR}$	4.65	3.96	3.70	2.39	1.80	1.70
C3	$R_{1DD}$	93.07	93.86	93.85	94.33	95.57	96.89
	$R_{1CSA}$	0.83	0.78	0.90	0.91	0.91	0.88
	$R_{1SR}$	6.10	5.36	5.25	4.76	3.52	2.23
C4	$R_{1DD}$	93.87	94.02	94.26	94.07	94.57	95.68
	$R_{1CSA}$	0.69	0.74	0.91	1.09	1.06	1.03
	$R_{1SR}$	5.44	5.24	4.83	4.84	4.37	3.29
C5	$R_{1DD}$	98.04	98.19	98.39	98.44	98.54	98.79
	$R_{1CSA}$	0.72	0.78	0.72	0.75	0.76	0.63
	$R_{1SR}$	1.24	1.03	0.89	0.81	0.70	0.58
<u>100.61 MHz</u>							
C1	$R_{1DD}$	51.91	53.06	58.62	63.92	67.66	70.40
	$R_{1CSA}$	35.81	36.67	33.05	30.43	29.08	26.13
	$R_{1SR}$	12.28	10.27	8.33	5.65	3.26	3.47
C2	$R_{1DD}$	53.98	55.31	57.81	65.10	72.05	75.15
	$R_{1CSA}$	33.59	34.76	33.69	30.02	24.38	21.80
	$R_{1SR}$	12.43	9.93	8.50	4.88	3.57	3.05
C3	$R_{1DD}$	48.48	50.71	53.53	58.04	62.01	66.17
	$R_{1CSA}$	35.19	34.46	34.00	31.62	30.61	29.21
	$R_{1SR}$	16.33	14.83	12.47	10.34	7.38	4.62
C4	$R_{1DD}$	50.83	49.04	50.61	51.76	53.62	57.77
	$R_{1CSA}$	32.88	35.28	37.10	37.73	36.87	35.20
	$R_{1SR}$	16.29	15.68	12.29	10.51	9.51	7.03
C5	$R_{1DD}$	75.61	77.16	80.85	80.88	82.19	83.87
	$R_{1CSA}$	22.02	21.11	17.77	17.91	16.84	15.25
	$R_{1SR}$	2.37	1.73	1.38	1.21	0.97	0.88

Unit: in %.

is responsible for the variation of the chemical shifts. A comparison of the chemical shifts of the carbon signals shows that the C-1, C-2, C-3, and C-4 atoms shift downfield with a temperature increase, whereas the C-5 signal shifts upfield. The reasons are given as follows:

1. C-1 and C-2 atoms are located on the main chain of the polymer; segmental motion at elevated temperature is inhibited due to the rigid conformation. Therefore, the shielding

tensors cannot be averaged out effectively. As a matter of fact, the distribution of the electron density is inhomogeneous; hence, C-1 and C-2 atoms shift to a lower field.

2. C-3 and C-4 atoms are located on the side chain, where the degree of motion is considerable more mobile than for the C-1 and C-2 atoms; however, it is not as flexible as for the C-5 atom. Therefore, the signals still shift slightly downfield.
3. The C-5 atom on the terminal of the side

**Table V** The Chemical Shifts of Poly(4-methyl-1-pentene) of Medium Molecular Weight

	358 K	363 K	373 K	383 K	393 K	403 K
<u>25.18 MHz</u>						
	42.21	42.23	42.31	42.36	42.44	42.51
	31.02	31.04	31.08	31.16	31.24	31.32
	45.91	45.92	45.95	45.97	46.02	46.04
	25.80	25.81	25.82	25.84	25.86	25.87
	23.73	23.72	23.71	23.69	23.67	23.65
<u>100.61 MHz</u>						
	42.24	42.29	42.40	42.47	42.53	42.60
	30.04	31.08	31.20	31.28	31.36	31.45
	45.90	45.93	46.00	45.03	46.06	46.10
	25.78	25.80	25.84	25.86	25.88	25.90
	23.70	23.69	23.69	23.66	23.64	23.61

Unit: measured in ppm.

chain and the carbon atoms of tetrachloroethane are freely rotatable. From the experimental data, we observed that the C-5 atom shifts slightly upfield with the temperature increase.

### $T_1$ and NOE

The longest  $T_1$  measured here is that of carbon atom C-5. It is easily explained by the free local motion of the terminal carbon atoms. Therefore, a longer  $\tau_c$  and a shorter  $T_1$  were obtained. (Table I). A further observation reveals that C-3 and C-4 atoms on the side chain have longer  $T_1$  than that of the C-1 and C-2 atoms on the main chain. The reason is that the rigid structure of the main chain has hindered the free motion of the carbon atoms.

According to theory, carbon atoms with the same chemical environment follow the following equation:  $T_1(\text{CH}) = 2 \times T_1(\text{CH}_2)$ . However, the ratio of the  $T_1$  of C-2 (CH) to that of C-1 (CH<sub>2</sub>) on the main chain gives  $T_1(\text{C-2})/T_1(\text{C-1}) = 1.72 \pm 0.08$ , whereas that of C-4 (CH) to C-3 (CH<sub>2</sub>) on the side chain equals  $T_1(\text{C-4})/T_1(\text{C-3}) = 2.42 \pm 0.16$ . Both ratios deviate from the standard value of 2. We can assume that the C-2 on the main chain is more rigid,  $\tau_c$  is longer, and  $T_1$  is shorter; therefore, the  $T_1$  ratio is less than 2. A comparison of the carbon atoms C-3 and C-4 shows that C-3 is more rigid and less flexible; here, the  $T_1$  ratio is larger than 2.

The study of the NOE values (Table II) reveals that the NOE of the C-5 atom is almost identical to the theoretical maximum value of 1.989. This in-

dicates that the C-5 atom undergoes purely <sup>13</sup>C—<sup>1</sup>H dipolar relaxation. It is not surprising since the C-5 atom has the largest number of neighboring protons, which makes  $T_{1\text{DD}}$  most effective. Besides, below the vaporization point, the C-5 atom rotates so fast that  $\tau_c$  becomes very short; as a result, the contribution of the spin rotation relaxation is negligible. Moreover, the fast rotation of the C-5 atom averages out the shielding tensors  $\delta_{\parallel}$  and  $\delta_{\perp}$ , and the chemical-shift anisotropic relaxation can be neglected as well.

From Table II, we found that at a lower temperature, such as 358 K, the NOE values of C-1 and C-4 atoms are larger than those of C-2 and C-3 atoms, respectively. However, at a higher temperature, such as 383 K, the situation reverses. This result suggests that the <sup>13</sup>C—<sup>1</sup>H dipolar relaxation is the dominant relaxation mechanism for C-2 and C-3 atoms at higher temperatures. The reason is rather complicated: As can be seen, the C-2 atom, located on the most rigid part of the polymer structure, is the least flexible. The local motion is not easily affected by the change of the temperature. Therefore, a dipole-dipole relaxation mechanism overwhelms. The same explanation can be applied to C-3 and C-4 atoms.

Generally, NOE values of all carbon atoms increase with temperature. This indicates that overall spin-lattice relaxation tends to follow a pure <sup>13</sup>C—<sup>1</sup>H dipolar relaxation mechanism with a temperature increase.

### Comparison of Several $T_1$ Models

In the present work, four kinds of mathematical models for the spin-lattice relaxation were applied to the simulation of poly(4-methyl-1-pentene). A brief review of the correlation functions is presented in the following:

#### The IR Model<sup>30</sup>

With the assumption of a pure dipolar relaxation mechanism, the spin-lattice relaxation rate can be expressed by the following equation:

$$R_{1\text{DD}} = \frac{1}{T_{1\text{DD}}} = \frac{\hbar^2 \gamma_C^2 \gamma_H^2}{10} \frac{1}{r_{\text{CH}}^6} (J(\omega_H - \omega_C) + 3J(\omega_C) + 6J(\omega_H + \omega_C)) \quad (9)$$

where  $\omega_H$  and  $\omega_C$  are the <sup>1</sup>H and <sup>13</sup>C Larmor frequencies.

The spectral density function is given by the following expression:



$$\begin{aligned}
 J(\omega) &= \int_{-\infty}^{\infty} K(\tau)e^{-i\omega\tau} d\tau \\
 &= \int_{-\infty}^{\infty} K(0)e^{-\tau/\tau_c}e^{-i\omega\tau} d\tau \\
 &= A(\tau_c/(1 + \omega^2\tau_c^2)) \quad (10)
 \end{aligned}$$

where  $k(\tau)$  is the corresponding correlation function.

**HH Model<sup>21</sup>**

The application of eq. (10) for polymer in solution is by far oversimplified. Hall and Helfand developed a modified version of the correlation function:

$$G(t) = \exp(-t/\tau_2)\exp(-t/\tau_1)I_0(t/\tau_1) \quad (11)$$

where  $I_0$  is the Bessel function of integral order zero, and  $\tau_2$  represents the correlation time for the single-bond conformational transitions and  $\tau_1$  is the correlation time for cooperative transitions.

The corresponding spectral density function is given by

$$\begin{aligned}
 J(\omega) &= 2\{((\tau_2^{-1})(\tau_2^{-1} + 2\tau_1^{-1}) - \omega^2)^2 \\
 &\quad + (2(\tau_2^{-1} + \tau_1^{-1})\omega)^2\}^{-1/4} \\
 &\quad \times \cos\left[\frac{1}{2} \arctan\left(\frac{2(\tau_2^{-1} + \tau_1^{-1})\omega}{\tau_2^{-1}(\tau_2^{-1} + 2\tau_1^{-1}) - \omega^2}\right)\right] \quad (12)
 \end{aligned}$$

Model	$r_0$	$\tau_2/\tau_1$	$\tau_1/\tau_0$	a
IR	0.068			
HH	0.049	1.51		
KKI	0.109		400.0	0.26
DLM	0.078	1.50	400.0	0.26

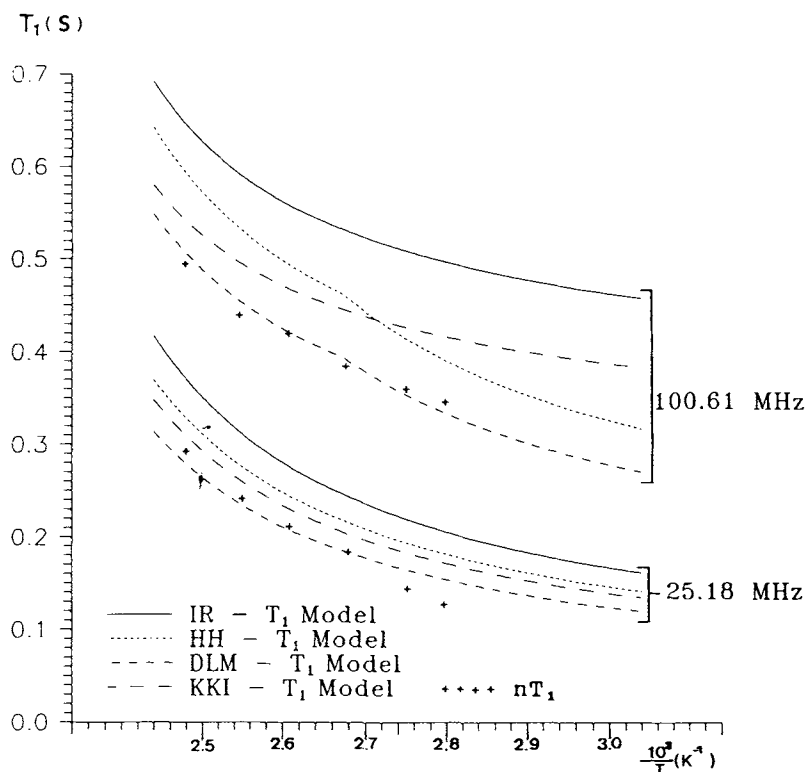


**Figure 2** Comparison of 25.18 MHz  $nT_1$  values for C-1 carbon of poly(4-methyl-1-pentene) with fitted parameters for the four models.

**KKI Model<sup>31</sup>**

The correlation function proposed by Kinoshita and co-workers can be written as follows:

$$G(t) = (1 - a)\exp(-t/\tau_1) I_0(t/\tau_1) + a \exp(-t/\tau_0) \quad (13)$$

where  $\tau_0$  is the correlation time of the local anisotropic reorientation, i.e., the bond liberation term. The Fourier transformation yields the spectral density:

$$J(\omega) = \frac{(1 - a)\tau_1}{1 + \omega^2\tau_1^2} + \frac{a\tau_0}{1 + \omega^2\tau_0^2} \quad (14)$$

and

$$1 - a = \left( \frac{\cos \theta - \cos^3 \theta}{2(1 - \cos \theta)} \right)^2 \quad (15)$$

where a random anisotropic fast reorientation of the CH vector inside a cone of half-angle  $\theta$  is proposed,<sup>32</sup> the axis of which is the rest position of the CH bond:

$$J_{HH}(\omega) = \frac{\tau_1}{1 + \omega^2\tau_1^2} \quad J_0(\omega) = \frac{\tau_0}{1 + \omega^2\tau_0^2}$$

The dipolar relaxation rate can then be expressed as

Model	$\tau_0$	$\tau_2 / \tau_1$	$\tau_1 / \tau_0$	a
IR	0.082			
HH	0.049	1.51		
KKI	0.124		400.0	0.20
DLM	0.089	1.50	400.0	0.20

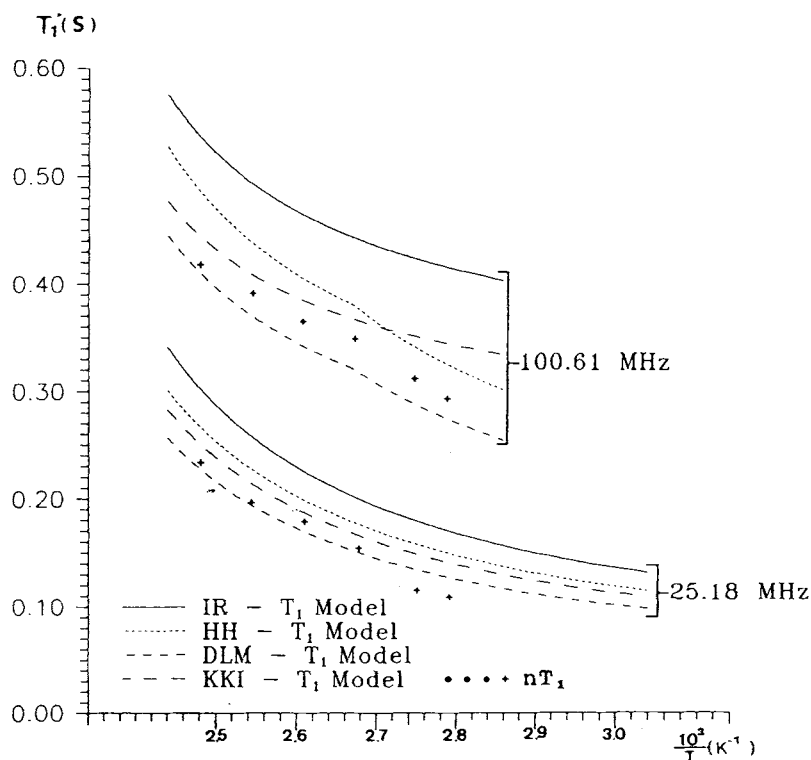


**Figure 3** Comparison of 25.18 MHz  $nT_1$  values for C-2 carbon of poly(4-methyl-1-pentene) with fitted parameters for the four models.

$$R_1 = \frac{1}{T_1} = (1 - a) \frac{\hbar^2 \gamma_C^2 \gamma_H^2}{10} \frac{1}{r_{CH}^6} [J_{HH}(\omega_H - \omega_C) + 3J_{HH}(\omega_C) + 6J_{HH}(\omega_H + \omega_C)] + a \frac{\hbar^2 \gamma_C^2 \gamma_H^2}{10} \frac{1}{r_{CH}^6} [J_0(\omega_H - \omega_C) + 3J_0(\omega_C) + 6J_0(\omega_H + \omega_C)] \quad (16)$$

$$G(t) = (1 - a) \exp(-t/\tau_2) \exp(-t/\tau_1) I_0(t/\tau_1) + a \exp(-t/\tau_0) \quad (17)$$

The spectral density function is

$$J(\omega) = \frac{1 - a}{(\alpha + i\beta)^{1/2}} + \frac{a\tau_0}{1 + \omega^2\tau_0^2} \quad (18)$$

**DLM Model<sup>33</sup>**

The DLM model describes the local chain motion in terms of conformational transitions  $\tau_2$  and the bond liberation  $\tau_0$ , which combines the HH and KKI models. The corresponding correlation function becomes

where  $\alpha = \tau_2^{-2} + 2\tau_1^{-1}\tau_2^{-1} - \omega^2$  and  $\beta = -2\omega(\tau_1^{-1} + \tau_2^{-1})$  and let

$$J_{HH}(\omega) = \frac{1 - a}{(\alpha + i\beta)^{1/2}}, \quad J_0(\omega) = \frac{\tau_0}{1 + \omega^2\tau_0^2}$$

Model	$\tau_0$	$\tau_2 / \tau_1$	$\tau_1 / \tau_0$	a
IR	0.054			
HH	0.039	1.52		
KKI	0.092		400.0	0.30
DLM	0.065	1.51	400.0	0.30

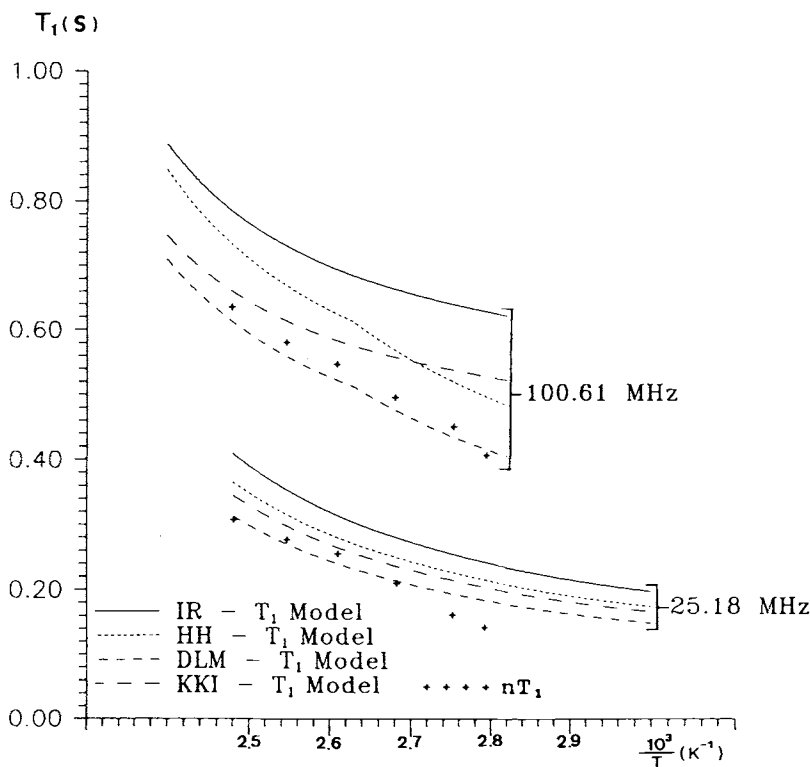


**Figure 4** Comparison of 25.18 MHz  $nT_1$  values for C-3 carbon of poly(4-methyl-1-pentene) with fitted parameters for the four models.

**Table VI** The Correlation Functions of Various  $T_1$  Models

$T_1$ Model	Correlation Function
IR	$r(t) = r_0 \exp(-t/\tau_1)$
HH	$r(t) = r_0 \exp(-t/\tau_2) \times \exp(-t/\tau_1) I_0(t/\tau_1)$
KKI	$r(t) = r_0 [(1-a) \exp(-t/\tau_1) + a]$
DLM	$r(t) = r_0 [(1-a) \exp(-t/\tau_2 - t/\tau_1) \times I_0(t/\tau_1 + a)]$

The spin-lattice relaxation rate of carbon nuclei can be expressed as in eq. (16). The results obtained with different models should be consistent with the experimental  $T_1$  and NOE values, where NOE is

defined as

$$\eta = \frac{\gamma_H}{\gamma_C} \frac{6J(\omega_H + \omega_C) - J(\omega_H - \omega_C)}{J(\omega_H - \omega_C) + 3J(\omega_C) + 6J(\omega_H + \omega_C)} \quad (19)$$

We have already verified that the  $T_1$  values are independent of the molecular weights. Therefore, we only compared the measured  $T_1$  values and NOE for polymers with medium molecular weight with the data obtained with the IR, HH, KKI, and DLM models.

Table VI presents the correlation functions for the relevant  $T_1$  models. By changing the corresponding parameters, we obtained the best-fitted curve and the parameter set (Figs. 2-6). The CH

Model	$r_0$	$\tau_2/\tau_1$	$\tau_1/\tau_0$	a
IR	0.045			
HH	0.031	1.52		
KKI	0.083		400.0	0.35
DLM	0.058	1.51	400.0	0.35

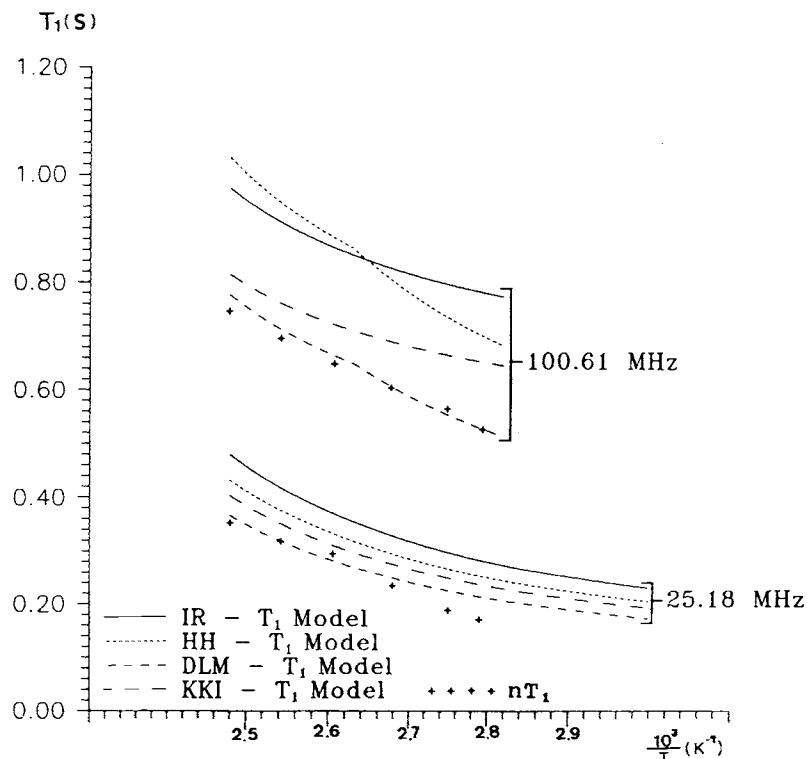


**Figure 5** Comparison of 25.18 MHz  $nT_1$  values for C-4 carbon of poly(4-methyl-1-pentene) with fitted parameters for the four models.

Model	$\tau_0$	$\tau_2/\tau_1$	$\tau_1/\tau_0$	$a$
IR	0.008			
HH	0.006	1.49		
KKI	0.017		400.0	0.45
DLM	0.012	1.48	400.0	0.45

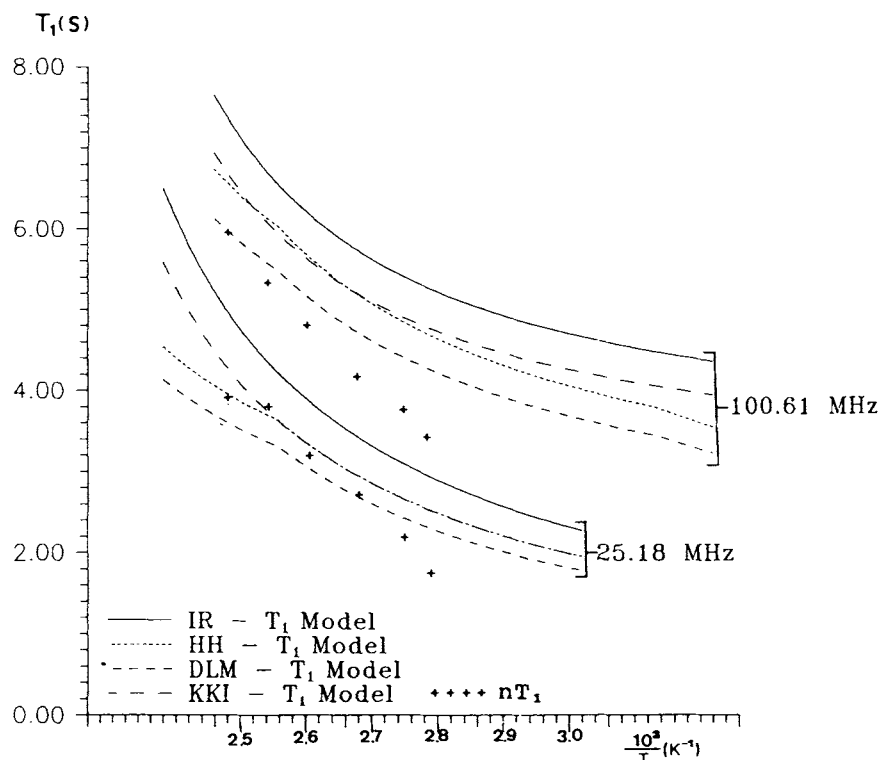


**Figure 6** Comparison of 25.18 MHz  $nT_1$  values for C-5 carbon of poly(4-methyl-1-pentene) with fitted parameters for the four models.

conic angles for all carbon atoms can be evaluated by eq. (15) (Table VII). In our studies, the DLM models give the best result.

Poly(4-methyl-1-pentene) is an oxygen-enriched substance. The paramagnetism of oxygen shortens the spin-lattice relaxation time. Using the DLM

model calculation, a smaller  $a$  value [eq. (15)] can be obtained for short  $T_1$ , which implies a smaller CH conic angle  $\theta$  for the carbon nuclei. As a result, there will be more free space for the side chain that allows oxygen to pass through more easily. However, as all the experiments in the present work were performed in a sealed degassed tube, this conclusion cannot be proven here.

**Table VII** The  $a$  Values and the CH Half-conic Angle for All Carbon Atoms of Poly(4-methyl-1-pentene)

	C <sub>1</sub>	C <sub>2</sub>	C <sub>3</sub>	C <sub>4</sub>	C <sub>5</sub>
$a$	0.26	0.20	0.30	0.35	0.45
$\theta$	25.4	21.9	27.5	30.2	35.2

### CONCLUSIONS

A few conclusions can be obtained from the NMR studies of the segmental motions of poly(4-methyl-1-pentene). First, the dominant spin-lattice relaxation mechanism of the polymer is the <sup>13</sup>C—<sup>1</sup>H di-

polar relaxation. Second, for polymers with a DP > 100, the  $T_1$  values and the NOE only depend on the molecular segmental motion. Third, the strength of the magnetic field affects the relaxation mechanism due to chemical-shift anisotropic effects.

For poly(4-methyl-1-pentene),  $\omega\tau_c < 1$ ,  $\tau_c$  decreases with increasing temperature; as a result,  $T_1$  increases. The  $T_1$  ratios for C-2 to C-1, as well as for C-4 to C-3, deviate from the expected value of 2. The reason can be explained by the different segmental motions for C-2 and C-4, as well as for C-1 and C-3.

A comparison of the  $T_1$  mathematical models reveals that the more factors considered for the calculation the more consistent are the results with the experimental  $T_1$  values. Among the four models, the DLM model evidently gives the best results.

The financial support of this research by the National Science Council, Republic of China, under the grant NSC81-0208-M006-20 is gratefully acknowledged. The authors wish to thank Professor J.-F. Kuo, National Cheng Kung University, for his helpful discussions.

## REFERENCES

- R. Kosfeld, C. Kreuzburg, and R. Krause, *Makromol. Chem.*, **189**, 2077 (1988).
- M. Koepf, G. Schnur, and R. Kimmich, *J. Polym. Sci. Part A Polym. Chem.*, **26**, 319 (1988).
- P. T. Callaghan, *Polymer*, **29**, 1951 (1988).
- R. Guyonnet and J. P. Cohen-Addad, *Macromolecules*, **22**, 135 (1989).
- M. M. Fuson and D. M. Grant, *Macromolecules*, **21**, 944 (1988).
- J. R. C. Van der Maarel, D. Lankhorst, J. De Bleijser, and J. C. Leyte, *Macromolecules*, **135**, 62 (1987).
- C. C. Hung, J. H. Shibta, A. A. Jones, and P. T. Inglefield, *Polymer*, **28**, 1062 (1987).
- H. C. Marsmann and E. Meyer, *Makromol. Chem.*, **188**, 887 (1987).
- C. J. M. Van Rijn, J. De Bleijser, and J. C. Leyte, *Macromolecules*, **20**, 1248 (1987).
- J. A. Ratto, P. T. Inglefield, R. A. Rutowski, K. L. Li, A. A. Jones, and A. K. Roy, *J. Polym. Sci. Part B Polym. Phys.*, **25**, 1419 (1987).
- P. Tekely, *Macromolecules*, **19**, 2544 (1986).
- C. J. M. Van Rijn, W. Jesse, J. De Bleijser, and J. C. Leyte, *J. Phys. Chem.*, **91**, 203 (1987).
- F. D. Blum, B. Durairaj, and A. S. Padmanathan, *J. Polym. Sci. Part B Polym. Phys.*, **24**, 493 (1986).
- R. Raghaven, T. L. Maver, and F. D. Blum, *Macromolecules*, **20**, 814 (1987).
- S. Pickup, F. D. Blum, W. T. Ford, and M. Periyasamy, *J. Am. Chem. Soc.*, **108**, 3987 (1986).
- J. Schaefer, E. O. Stejskal, and R. Buchdahl, *Macromolecules*, **10**, 384 (1977).
- H. Yamamoto, F. Horii, and H. Odani, *Macromolecules*, **22**, 4130 (1989).
- A. Hirai, F. Horii, R. Kitamaru, T. Ito, K. Kobayashi, and H. Sumitomo, *Macromolecules*, **23**, 1837 (1990).
- C. M. Hu and W. Y. Chiang, *J. Polym. Sci. Part A: Polym. Chem.*, **191**, 681 (1990).
- A. Sebenik, U. Osredkar, and M. Lesar, *Polymer*, **31**, 130 (1990).
- C. K. Hall and E. Helfand, *J. Chem. Phys.*, **77**, 3275 (1982).
- J. L. Viovy, L. Monnerie, and J. C. Brochon, *Macromolecules*, **16**, 1845 (1983).
- A. A. Jones and W. H. Stockmayer, *J. Polym. Sci. Polym. Phys. Ed.*, **15**, 847 (1975).
- J. Skolnick and R. Yaris, *Macromolecules*, **16**, 266 (1983).
- A. Allerhand and R. K. Hailstone, *J. Chem. Phys.*, **56**, 3718 (1972).
- C. Chachaty, A. Forchioni, and J. C. Ronfard-Haret, *Makromol. Chem.*, **173**, 213 (1973).
- E. Helfand, *J. Chem. Phys.*, **54**, 4651 (1971).
- F. A. Bovey, *Nuclear Magnetic Resonance Spectroscopy*, Academic Press, New York, 1988, pp. 261–262.
- R. J. Abraham and P. Loftus, *Proton and Carbon-13 NMR Spectroscopy, an Integrated Approach*, Heyden & Son, Ltd., London, 1978, pp. 130–134.
- F. Perrin, *Ann. Phys.*, **12**, 169 (1929).
- K. Kinoshita, S. Kawato, and A. Ikegami, *Biophys. J.*, **20**, 289 (1977).
- R. Dejean de la Batie, F. Laupretre, and L. Monnerie, *Macromolecules*, **21**, 2052 (1988).
- R. Dejean de la Batie, F. Laupretre, and L. Monnerie, *Macromolecules*, **21**, 2045 (1988).

Received April 26, 1993

Accepted September 14, 1993